Evaluation of U-Net3+ and Attention U-Net for Solar Energy Estimation on Urban Rooftops using LiDAR DSMs

Maryam Hosseini, Sina Irannejad, Hossein Bagheri*
Faculty of Civil Engineering and Transportation, University of Isfahan, h.bagheri@cet.ui.ac.ir

Keywords: Solar Energy Potential Map, Solar Panel Placement, Deep Learning, U-Net Architecture, LiDAR DSM.

Abstract

This study investigates the feasibility of employing deep learning models, specifically the U-Net3+ and Attention U-Net architectures, to estimate annual solar energy potential maps (ASM) using high resolution LiDAR-derived digital surface models (DSMs). As urban areas increasingly seek sustainable energy solutions, precise localization of rooftop solar panels becomes essential. While accurate, traditional physical models, such as the Area Solar Radiation (ASR) model, are often computationally intensive and time consuming, limiting their application over large areas. This research proposes a novel framework that integrates deep learning techniques to enhance the efficiency and accuracy of solar energy potential estimation. The methodology includes data collection, generation of reference ASMs from LiDAR DSMs using the ASR model, and training various U-Net models on patches of DSM data. The U-Net 3+ model demonstrated the highest correlation with reference ASMs with an RMSE of 94.353 ($\frac{MWh}{m^2}$) and R^2 of 0.91, indicating its effectiveness in capturing the spatial relationships between topographical features and solar radiation. The results suggest that deep learning models can be a viable alternative to traditional physical models, facilitating quicker and more reliable solar energy potential mapping.

1. Introduction

Economic development and population growth have increased the demand for fossil fuels to supply electrical energy (Enerdata, 2018). The extraction, transportation, and combustion of fossil fuels have numerous environmental consequences. Utilizing renewable energy sources presents an effective solution to meet this demand while mitigating environmental impacts. Among renewable energy sources, solar energy has garnered particular attention due to its widespread availability, and installing solar panels in areas lacking access to electricity can effectively address power supply challenges (Zhong & Tong, 2020). The need for extensive areas to establish large solar power plants, along with the costs associated with transmitting energy to consumption sites, typically building blocks in urban areas, has led to an increasing focus on decentralized electricity generation from the solar energy potential captured by solar panels installed on building rooftops (Cucchiella et al., 2015; Lee et al., 2018). Numerous studies have been conducted regarding the site selection for installing solar panels on building roofs (Huang et al., 2015; Srećković et al., 2016). However, the site selection for installing solar panels in urban areas presents numerous challenges (An et al., 2023). Thus, accurately estimating the solar energy potential received by building rooftops is essential due to the costs associated with procuring, installing, and maintaining solar panels.

Various modelling techniques have been developed to estimate solar irradiance, broadly falling into two categories: empirical and physical models. Empirical models establish statistical correlations between irradiance and meteorological parameters such as cloud cover, temperature, and humidity (Besharat et al., 2013). In contrast, physical models simulate the radiative transfer process based on the geometric relationship between the Sun and the Earth, incorporating factors like solar altitude, azimuth, and the Earth-Sun distance (Jung et al., 2019). Numerous physical models have been applied to estimate solar energy potential (Dubayah & Rich, 1995; Fu, 2000; Hetrick et al., 1993; Miklánek, 1993; Prodanovic, 2002). These typically utilize topographic parameters derived from Digital Elevation Models (DEMs)—such as slope, aspect, and shadow casting—to calculate incident solar radiation. One widely recognized physical model is the Area Solar Radiation (ASR) tool within ArcGIS Pro. Several studies have validated its high accuracy against ground-based measurements (Kausika & Van Sark, 2021; Šúri & Hofierka, 2004). The accuracy of solar potential maps generated by these models is directly influenced by the spatial resolution of the input DEM. While freely available global Digital Surface Models (DSMs), such as SRTM and ASTER, are commonly used for this purpose, their inherent resolution and accuracy are often insufficient for detailed urban applications (Hosseini & Bagheri, 2025). Although various techniques have been proposed to enhance the accuracy of these DEMs, they cannot improve the spatial resolution (Bagheri et al., 2014, 2017a,b; Okolie et al., 2024). Consequently, a critical limitation persists in producing high-resolution Annual ASMs in complex urban environments for precise solar panel placement. In this context, high-resolution DSMs derived from airborne LiDAR have demonstrated exceptional capability for accurate solar energy estimation (Nelson & Grubesic, 2020; Polo & García, 2023), offering a potential solution to the resolution limitations of satellite-derived models.

Physical models such as ASR can estimate solar radiation at rooftops from LiDAR data. However, the ASR model, like other solar irradiance estimation models, requires significant computation time to produce solar energy potential maps due to its consideration of shading effects and related calculations for each point on the surface. As the spatial resolution of the DSM input increases, the time required to generate solar energy potential maps rises substantially.

Recently, several studies have employed deep learning models, which consider spatial correlations due to their convolutional structure, as suitable alternatives to statistical and physical models for estimating target parameters (Heo et al., 2020; Li et al., 2024). In previous studies, deep learning models have typically been employed to extract building boundaries or identify (classify) suitable buildings for solar panel installation

* Corresponding author

https://doi.org/10.5194/isprs-annals-X-4-W8-2025-379-2026 |

(Ren et al., 2022; Zhong et al., 2021). However, in some studies, the use of deep learning models to estimate solar irradiance has been limited to weather station data without considering the topographic effects of the surface, such as slope and aspect, as well as the surrounding topographical influences (Kaba et al., 2018; Kumari & Toshniwal, 2021). In literature, few studies have employed deep learning models to estimate solar irradiance received by surfaces, utilizing DSMs as the sole input data. For example, Heo et al. used a Convolutional Neural Network (CNN) based on DSMs to estimate the annual average solar energy potential received by surfaces. They concluded that the developed deep learning model effectively captured adjacent lands' topographic complexity and regional features, accurately estimating the annual average solar energy potential (Heo et al., 2020).

Considering the significance of topographical data in estimating the solar radiation received at the surface (Wang & Wang, 2015), along with the high computational costs associated with physical models for generating high resolution solar potential maps, this study investigates the feasibility of employing deep learning models to estimate solar energy potential using high resolution LiDAR data, based on physical models such as ASR model. The main objective of this research is to evaluate the potential of substituting physical models with deep learning models to produce high resolution solar energy potential maps at the urban level, thereby facilitating the optimal placement of solar panels on building rooftops. To achieve this, deep convolutional networks based on the U-Net architecture, employing topographical data obtained from LiDAR in an urban area, will be utilized to estimate annual solar radiation.

2. Study Area & Dataset

In this study, the central area of Amsterdam, as illustrated in Figure 1, was selected as the study area. Amsterdam is the capital of the Netherlands, located in North Holland province in the western part of the country, situated in the Amstel River delta. It predominantly features low-lying topography, with an average elevation of approximately 2 m above sea level. As a result, the natural landscape of Amsterdam and its surrounding regions generally lack significant elevation changes or steep slopes. Influenced by its proximity to the North Sea, the city experiences a maritime climate characterized by mild temperatures, relatively high humidity, cool summers, and moderate winter. Despite its flat topography, the city's orientation of buildings, streets, and waterways can impact factors such as solar exposure, wind patterns, and microclimatic conditions in specific areas. Therefore, the strategic placement of solar panels on building rooftops for this study area is of considerable importance.

This study uses the DSM derived from LiDAR data with a spatial resolution of 0.5 m as input for the deep learning based solar radiation prediction models. This DSM is sourced from the third version of the Actueel Hoogtebestand Nederland (AHN3), collected by Publieke Dienstverlening Op de Kaart (PDOK), and is freely available to the public. The AHN3 DSM consists of raw raster data with grid intervals of 0.5 m, derived from LiDAR point cloud data at the exact spatial resolution, without further modifications. The AHN3 data were collected between 2014 and 2019.

3. Method

Figure 2 illustrates the proposed framework for generating annual average solar energy potential maps (ASM) of 2021, utilizing the LiDAR DSM and deep learning models based on the U-Net architecture. This framework comprises several stages, including data collection, generation of reference ASM from LiDAR DSM

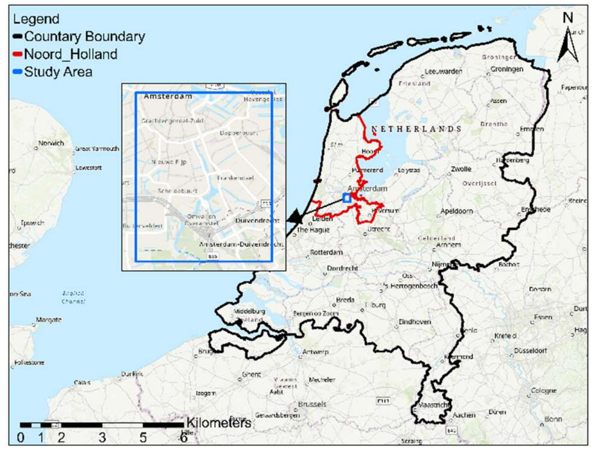

Figure 1. A view of the study area, part of Amsterdam, located in North Holland province, Netherlands.

using the ASR model, preparation of data for deep learning, model evaluation, and selection, predicting the ASM using the selected deep learning model, and the placement of solar panels on rooftops using the achieved ASM. Initially, a LiDAR DSM with a spatial resolution of 0.5 m covering the study area of Amsterdam was prepared. Subsequently, the ASR model estimated the ASM at the same resolution as the LiDAR DSM, resulting in a reference LiDAR ASM. After providing the LiDAR DSM and its corresponding reference ASM, data preparation for deep learning involved generating patches of 128 × 128 pixels with a resolution of 0.5 m. By determining the proportions of training, testing, and validation data, the deep learning models, including U-Net, Attention U-Net, and U-Net 3+, were trained using the LiDAR DSM patches as input and the corresponding LiDAR-derived ASMs as labels. The evaluation of models was a thorough process involving calculating and comparing the accuracy of the deep learning models in producing ASM from the LiDAR DSMs. The selected model (UNet 3+) utilized all produced patches of LiDAR DSM to predict the LiDAR ASM of the study area. By mosaicking the predicted LiDAR ASM patches generated by the selected deep learning model, the predicted ASM was obtained. In the subsequent step, the accuracy of the predicted ASM was assessed against the reference LiDAR ASM derived from the ASR model. Finally, rooftop solar panel placement was conducted using the predicted ASM from the deep learning model compared to the reference ASM generated by the ASR model.

3.1 Area Solar Radiation

Solar radiation reaching the Earth's surface is influenced by atmospheric conditions, topography, and surface characteristics as it passes through the atmosphere. Solar radiation is categorized into three main types: direct, diffuse, and reflected radiation. Direct radiation constitutes the most significant portion of total solar radiation, reaching the Earth unobstructed from the Sun. Diffuse radiation, the second most significant component of total solar radiation, is scattered by atmospheric elements such as clouds and dust. Reflected radiation originates from surfaces on the Earth and typically contributes a minor share to total radiation, except in areas with highly reflective surfaces, such as snow. In the solar radiation estimation model within the Area Solar Radiation module of ArcGIS Pro, reflected radiation is not

https://doi.org/10.5194/isprs-annals-X-4-W8-2025-379-2026

included in the total radiation calculations; thus, total radiation is computed as the sum of direct and diffuse radiation (Fu, 2000).

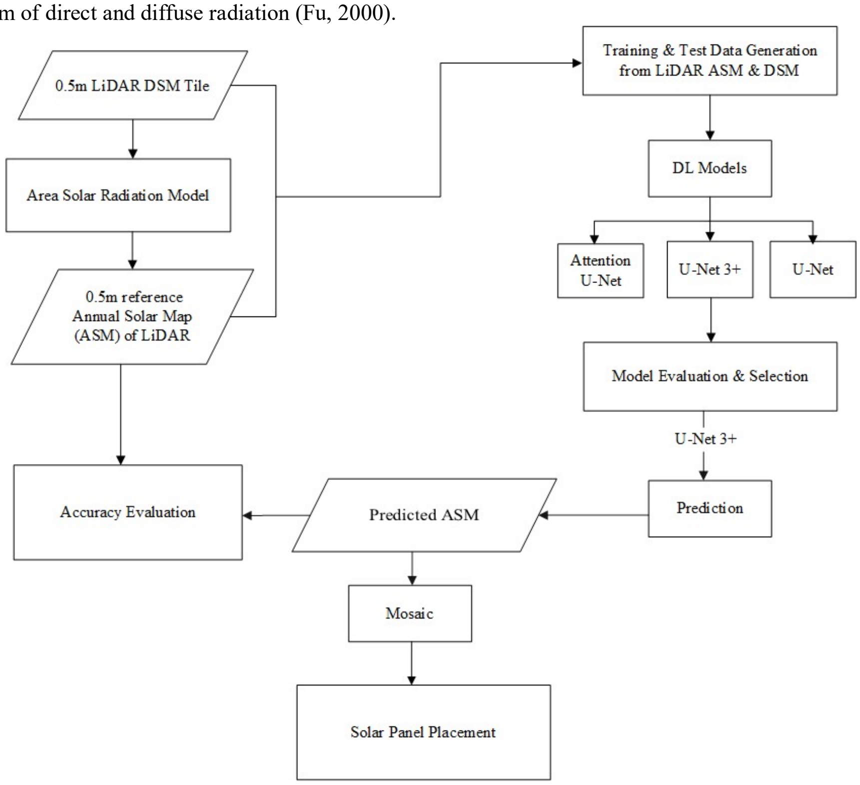

Figure 2. The proposed framework for generating the ASM from LiDAR DSM using the suggested deep learning models.

In this study, the ASM for 2021 was generated from LiDAR DSM tile with a spatial resolution of 0.5 m using the solar radiation estimation model available in the Area Solar Radiation module of ArcGIS Pro.

3.2 Utilizing Deep Learning for Solar Radiation Estimation

This research investigates the feasibility of replacing traditional physical models with U-Net models for estimating solar energy potential from high resolution LiDAR DSM data. U-Net and its improved variants (such as Attention U-Net and U-Net 3+) offer numerous advantages when working with DSM data (Ronneberger et al., 2015). These models can extract detailed information regarding the terrain topography from LiDAR DSM data and utilize this information to estimate solar energy potential. Thanks to the convolutional structure of these networks and their ability to comprehend spatial relationships among pixels in DSM, the U-Net model can harness the spatial correlations present in three-dimensional LiDAR data to provide more accurate estimates of solar energy potential. Skip connections between the encoder and decoder layers enhance the model's ability to capture spatial relationships relevant to solar energy potential maps, resulting in higher-precision outputs. Furthermore, the U-Net model's capability to handle sizeable high-resolution datasets, such as LiDAR DSM data, increases computational efficiency, producing higher-quality solar energy potential maps.

3.2.1 U-Net and its Variants: The U-Net architecture was introduced in 2015 and has become one of the most renowned architectures for semantic segmentation, initially designed for segmenting biomedical images (Ronneberger et al., 2015). UNet features a U-shaped structure comprising the Encoder (Downsampling) and the Decoder (Upsampling). This structure

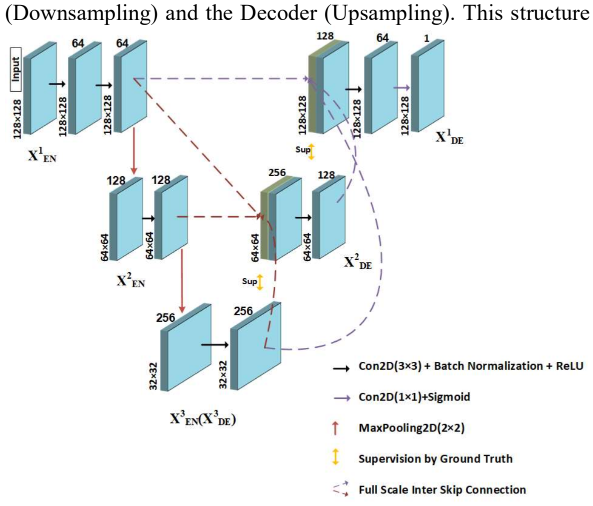

Figure 3. The structure of the U-Net 3+ network utilized in this study.

allows the network to learn and combine features at various levels. The Encoder comprises convolutional layers and pooling operations that extract significant features from the image at different levels while progressively reducing the spatial dimensions. In contrast, the Decoder increases the image dimensions using techniques such as upconvolution and concatenation. In other words, it reconstructs the image by utilizing the features learned from the Encoder and focusing on preserving critical details. Skip connections between the Encoder and Decoder facilitate the direct transfer of spatial information from the Encoder layers to the Decoder layers, thereby aiding in the accurate recovery of image features. This design enhances the model's ability to produce high-quality outputs, making U-Net particularly effective for tasks that require precise localization and segmentation.

The Attention U-Net network is a recent advancement of the U-Net architecture that employs an attention mechanism (Shen et al., 2018) to enhance the network's performance and accuracy and improve detail recovery. In the Attention U-Net model, attention gates are utilized in the skip connections, allowing the network to automatically focus more on important details and significant regions of the image, thereby utilizing more relevant and meaningful information for processing. This enables the network to learn more complex and significant patterns from the data.

U-Net 3+ was introduced in 2020 as another improved version of U-Net (Huang et al., 2020). The architecture of this network incorporates dense and nested skip connections, as well as deep supervision, since the combination of multi-scale features is crucial for accurate segmentation. As Figure 3 illustrates, full-scale skip connections merge low-level details with highlevel semantic information from feature maps at various scales. In other words, the model receives feature maps of similar and smaller scales from the Encoder and obtains larger-scale feature maps from the Decoder. Meanwhile, deep supervision facilitates learning hierarchical representations from the collected feature maps at full scale. Specifically, the model receives a side output at each decoder level, monitored by reference data.

3.2.2 Experimental Setup and Performance Evaluation: Defining the training, validation, and test datasets to train U-Net models is essential. In this study, a LiDAR DSM tile, measuring 12,500 × 10,000 pixels at a resolution of 0.5 m, covered the study area was employed. After generating the corresponding ASM using the ASR model from the DSM, 7,566 patches with size 128 × 128 pixels were extracted from the DSM and the corresponding ASM. 80% of the total patches (4841 patches) were selected as the training dataset, while the remaining 20% (1514 patches) were set aside for testing. Additionally, 20% of the training dataset (1211 patches) was allocated for validation. The optimal structure of the various U-Net networks, including the number of layers and filters, was determined through training and evaluating the performance on the validation dataset. Figures 3 illustrate the design details for each architecture. All three networks were trained with a batch size of 32 for 300 epochs, utilizing an early stopping mechanism during the training process. Since U-Net networks were initially designed for segmentation tasks, the loss function in the final layer needed to be modified for regression applications. In this study, to adapt U-Net networks for estimating solar energy potential from DSM data in a regression framework, the Mean Squared Error (MSE) loss function was employed.

After training and evaluating the U-Net models on the training and validation datasets and finalizing the weights, the tuned networks estimated the ASM using patches of LiDAR DSM from the test dataset during the prediction phase. Several evaluation metrics were utilized to assess the accuracy of the U-Net-based deep learning models in the training and testing processes. RMSE and MAE were calculated as the root mean squared error and the mean absolute error, respectively, between the predicted ASM from the U-Net-based models and the reference ASM generated by the ASR model. Also, the coefficient of determination, R^2, quantifies the correlation between the predicted ASM and the reference ASM.

3.3 Solar Panel Placement

The placement of solar panels on rooftops requires high resolution solar energy potential maps. U-Net models facilitate the generation of solar energy potential maps corresponding to the resolution of input data (LiDAR DSM). This study evaluates the capability of the predicted ASM (generated by the U-Net 3+ deep learning model) in identifying suitable locations for solar panel installation. To achieve this, the generated ASM patches for the study area were mosaicked and integrated. Additionally, the building footprints provided by the OpenStreetMap (OSM) platform were utilized to determine the positions of the buildings. To assess the predicted ASM's ability to identify suitable locations for solar panel installation on rooftops, the annual average solar energy potential received by rooftop cells of each building was first calculated and converted to $\frac{KWh}{m^2}$. Subsequently, the following three conditions were considered:

1. Rooftop area requirement: Rooftops must have a minimum area of 30 m^2, as installations smaller than this are economically unfeasible for solar panel placement.

2. Roof slope calculation: The slope of the rooftops was calculated, ensuring it does not exceed 45̊. To achieve this, a slope layer was derived from LiDAR DSM data.

3. Roof orientation assessment: The orientation of the rooftops was evaluated to avoid north-facing roofs (22.5̊ < Aspect < 337.5̊), as these receive less sunlight in the Northern Hemisphere. This layer was also generated using LiDAR DSM data. These three criteria were applied to the solar potential layer to identify suitable locations for solar panel installations.

4. Result

4.1 Performance Evaluation of Deep Learning Models in Estimating ASM

The deep learning models based on U-Net, including ordinary U-Net, Attention U-Net, and U-Net 3+, were trained using pairs of LiDAR DSM and reference LiDAR ASM patches with a spatial resolution of 0.5 m. Table 1 compares the performance of the U-Net-based deep learning models against the ASR model in generating ASM from LiDAR DSM. The U-Net 3+ model exhibited the best performance in both the test and train sets, while the U-Net model demonstrated the weakest performance. In other words, the ASM estimated from LiDAR DSM using the U-Net 3+ model shows lower error (and thus more remarkable similarity) compared to the ASM generated by the U-Net and Attention U-Net models when assessed against the reference ASM produced by the ASR model. This highlights the effectiveness of the U-Net 3+ model in accurately predicting solar radiation potential from high resolution LiDAR DSM data.

Figure 4 displays the absolute error map of the ASM generated by the U-Net 3+ deep learning model compared to the reference ASM. In most areas of the study region, the absolute error values are very low and close to zero. However, as the slope of the surface increases, the absolute error also increases, reaching a maximum value of 1031.48 $\frac{KWh}{m^2}$ in tiny areas. These areas are primarily located in shadows cast by tall buildings. In other words, the ASR model that produced the reference ASM

https://doi.org/10.5194/isprs-annals-X-4-W8-2025-379-2026

accounted for sky and sun maps and the shading effects created by surrounding topography for each pixel. In contrast, although the U-Net 3+ model employs a convolutional structure and considers spatial relationships and the influence of adjacent topography in estimating solar energy potential, accuracy diminishes in regions with significant slope variations. Nevertheless, it is worth noting that these locations are outside building rooftops, and this research focuses on estimating solar radiation received by building rooftops.

Model	Train			Test		
	R^2	RMSE ($\frac{KWh}{m^2}$)	MAE ($\frac{KWh}{m^2}$)	R^2	RMSE ($\frac{KWh}{m^2}$)	MAE ($\frac{KWh}{m^2}$)
U-Net	0.88	108.357	68.781	0.81	138.525	79.422
Attention U-Net	0.92	84.254	53.695	0.86	119.698	72.390
U-Net 3+	**0.94**	**76.280**	**47.701**	**0.91**	**94.353**	**59.052**

Table 1. Performance evaluation of U-Net models in estimating ASMs from LiDAR DSM compared to reference ASM derived from ASR.

4.2 Results of Solar Panel Placement using the ASM Generated by U-Net 3+ compared to the ASR model

One of the objectives of this paper is to substitute deep learning models for physical models in estimating solar energy potential, focusing specifically on rooftops for solar panel placement. To evaluate the accuracy of solar energy potential estimation by the U-Net 3+ model, Figure 5 presents several example patches of predicted ASM (selected from test data) by the U-Net 3+ model in comparison with their corresponding reference ASM (generated by the ASR model) for rooftops in residential areas. The blue lines represent the building footprints. As can be observed, the ASM produced by the U-Net 3+ model closely resembles the reference ASM, which is further corroborated by the metrics provided for the test data in Table 1.

Next, a quantitative assessment of the quality of predicted ASM for the rooftop solar panel placement was conducted. Using building footprints, the reference and predicted annual average solar energy potential for the rooftops was extracted. Figure 6 illustrates the scatter plot of the annual average solar energy potential received by the roof of each building based on the reference and predicted ASM. The plot indicates a high correlation ($R^2 = 0.97$) between the annual average solar energy potential received by each building's roof based on the predicted ASM and the reference ASM. Additionally, with reported RMSE (25.63 $\frac{KW}{m^2}$) and MAE (18.77 $\frac{KW}{m^2}$) values, the annual average solar energy potential received by each building's roof, estimated by U-Net 3+, demonstrates a high level of accuracy.

In Figure 7, the rooftop solar potential map for some example buildings designated for solar panel installation is displayed based on the annual average solar energy potential received by the rooftops. The maps shown in Figure 7 present the values of the annual average solar energy potential received by the rooftops generated by the ASR model (a) and the U-Net 3+ model (b). The predicted values (by the U-Net 3+ model) for the annual average solar energy potential received by rooftops range from 0 to 906.1 $\frac{KWh}{m^2}$, while the estimates provided by the ASR model range from 0 to 931.7 $\frac{KWh}{m^2}$. The predicted values are, on average, 25.6 $\frac{KW}{m^2}$ lower than those generated by the ASR model. In other words, the rooftop solar potential map produced based on the predicted ASM by the U-Net 3+ model underestimates the solar energy potential. Nevertheless, Figure 6 shows a strong correlation between the predicted ASM and the reference ASM in the context of locating solar energy panels on building rooftops.

5. Discussion

One of the crucial factors in preparing solar energy potential maps, particularly at large scales such as cities with high spatial resolution (for the placement of solar panels on building rooftops), is the time required for estimating solar energy potential. Table 2 presents the time needed for the deep learning models U-Net, U-Net 3+, and Attention U-Net in both training and predict modes, as well as the physical model ASR, for estimating the annual average solar energy potential of patches covering the study area (7,566 patches of 128 × 128 pixels at a resolution of 0.5 m). The physical ASR model can accurately estimate solar energy potential maps for all patches within the study area; however, the time required for ASM generation using this model exceeds 14 hours and 24 minutes. Consequently, utilizing the ASR model for estimating solar energy potential maps entails significantly higher computational and temporal costs than U-Net-based models. This renders the ASR model inefficient for extensive areas, particularly at high spatial and temporal resolutions. Thus, the ASR physical model is suitable for generating solar energy potential maps for a smaller area. Subsequently, the U-Net-based models can be trained on these maps, allowing for estimating solar energy potential across an extensive region.

As indicated, the time required for training the U-Net model is less than other models; however, according to Table 1, it achieves significantly lower accuracy than the U-Net 3+ and Attention U-Net models. Therefore, despite the reduced training time for the U-Net model, its performance in estimating solar energy potential diminishes due to its lower accuracy than the other models. U-Net 3+ necessitates considerably more training time among the deep learning models due to its Full-Scale Connected architecture and supervised learning across different scales. Although the training time is increased compared to Attention U-Net, this technique improves accuracy in estimating solar energy potential. Nevertheless, the performance of the Attention U-Net model is comparable to that of the U-Net 3+ in terms of accuracy. It is noteworthy that the U-Net 3+ model and its more complex architecture than the other two U-Net models have undergone more training epochs, further influencing the time required.

Another critical factor in comparing the performance of the models is their processing and estimation speed during the deployment phase. The deep learning models U-Net and Attention U-Net can estimate the annual average solar energy potential for all patches of the LiDAR DSM covering the study area in less than 3 seconds, while the estimation time for the U-Net 3+ model is approximately 25 seconds. Therefore, when estimating the annual average solar energy potential over large areas, if time is of greater importance and a slight compromise on accuracy is acceptable, the Attention U-Net model can be a suitable alternative to the physical model. However, considering the parameter of accuracy and the necessity for more precise estimates, it is noteworthy that the estimation time for solar energy potential using the U-Net 3+ model is also within the scale

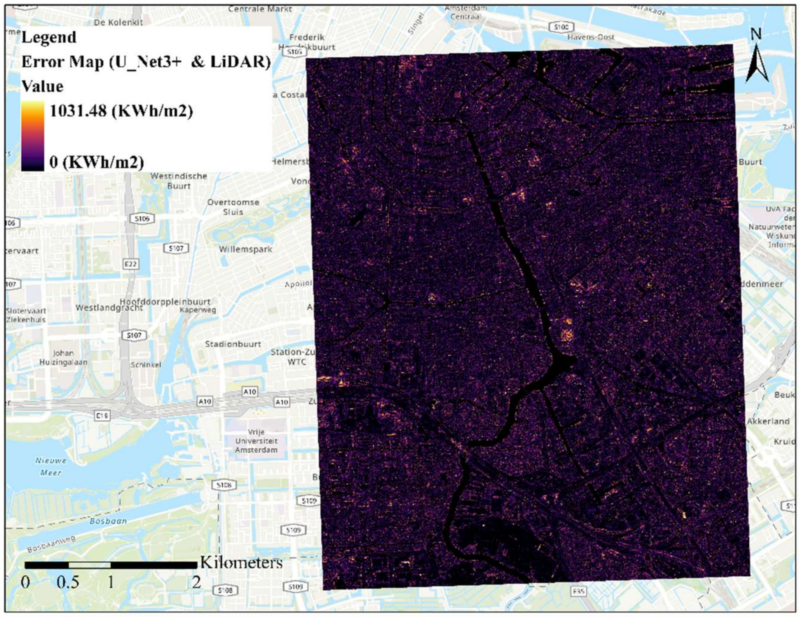

Figure 4. The absolute error map between predicted ASM (generated by the U-Net 3+) and reference ASM (generated by the ASR model).

Model	Training Time	Predicted Time	Total Time
ASR Model	-	-	14h 24m 26s
U-Net	0h 25m 46s	2.86s	0h 25m 48.86s
U-Net 3+	3h 39m 19s	24.37s	3h 39m 43.37s
Attention U-Net	0h 42m 29s	2.77s	0h 42m 31.77s

Table 2. The time required by U-Net models and the ASR model to estimate the annual average solar energy potential for the patches covering the study area.

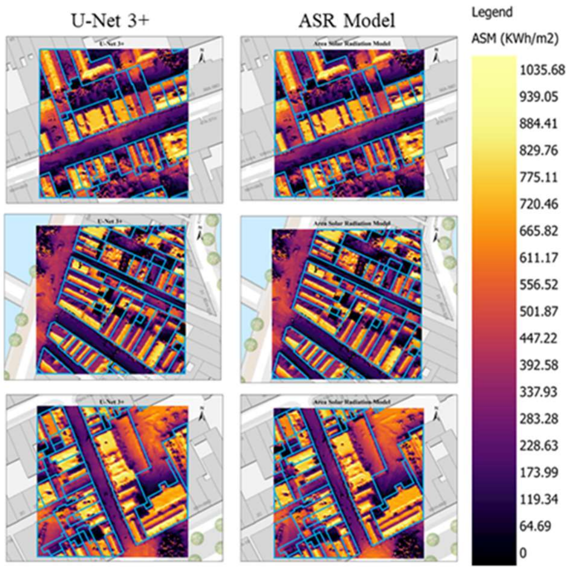

Figure 5. The ASMs generated by the U-Net 3+ model (left) and the ASR model (right) for selected sample data from residential buildings in the study area.

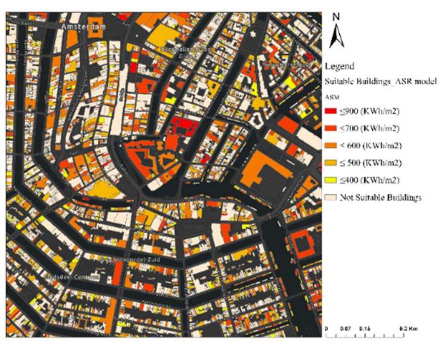

a) Reference ASM (generated by ASR Model)

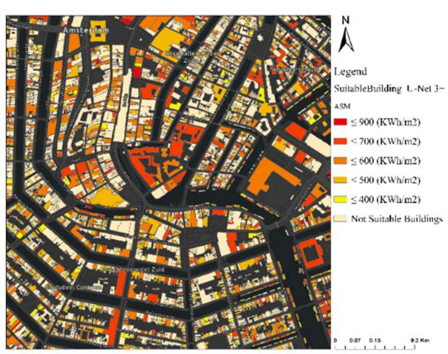

b) Predicted ASM (generated by U-Net 3+ Model)

Figure 7. Maps of building suitability for solar panel installation based on the annual average solar energy potential received by rooftops, generated by the ASR model (a) and the U-Net 3+ model (b).

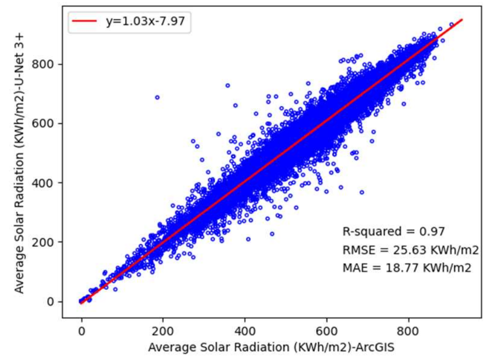

Figure 6. The performance of the U-Net 3+ model in predicting the annual average solar energy potential received by each building's rooftop.

of seconds. This makes the U-Net 3+ model a viable option for generating ASM maps for the placement of solar panels, as it not only reduces processing time compared to the ASR physical model but also provides an efficient alternative to traditional physical models, thereby decreasing the overall processing time required for the preparation of ASM maps.

6. Conclusion

Solar energy utilization in urban areas requires precise localization of rooftop solar panels. Achieving this goal necessitates high resolution solar energy potential maps. Physical models for estimating solar radiation, such as the ASR model, require high resolution DSMs like LiDAR DSMs to produce such maps. However, using physical models, ASM estimation based on high resolution LiDAR DSMs demands more time and computational cost. Thus, applying these models to produce solar energy potential maps for extensive areas, particularly at high spatial and temporal resolutions, becomes tricky.

This study proposed a practical framework for estimating the ASM using U-Net models. It was realized by training and testing various U-Net models, including U-Net, Attention U-Net, and U Net 3+, using the LiDAR ASM generated by the ASR model and high resolution (0.5 m) LiDAR DSM data. After assessing the accuracy of these models, U-Net 3+ was selected as the most accurate model compared to the reference ASM generated by the ASR model. The results demonstrated that deep learning models based on CNN structure, such as U-Net 3+, could explore the spatial relationship between neighborhood topographies, providing comprehensive insight into the impact of topography on solar radiation estimate using convolutional operations. In this way, they can manage large datasets with high resolution, such as LiDAR DSM data, resulting in the generation of solar energy potential maps that closely resemble reference solar energy potential maps produced by the ASR model. Therefore, these models can be a suitable alternative to physical models.

Subsequently, the identification of suitable buildings for solar panel installation was evaluated using the ASM estimated by the U-Net 3+ model compared to the reference ASM derived from the ASR model. The results indicated a remarkably high correlation between the predicted ASM and the reference ASM in locating solar energy panels on the rooftops of buildings. This high correlation instills confidence in the accuracy of our results and the potential of our approach to estimating ASMs using high resolution LiDAR DSMs in much less time compared to the physical solar radiation estimation models such as the ASR model.

For future research, developing a deep learning framework capable of directly identifying suitable rooftop locations for solar panel installation using high resolution LiDAR data as input is suggested, enabling the model to autonomously determine optimal solar panel installation areas.

Acknowledgements

We would like to express our gratitude to OpenStreetMap for providing essential geospatial data and AHN for supplying the Amsterdam LiDAR data.

References

An, Y., Chen, T., Shi, L., Heng, C. K., Fan, J., 2023. Solar energy potential using GIS-based urban residential environmental data: A case study of Shenzhen, China. *Sustainable Cities and Society*, *93*, 104547. https://doi.org/10.1016/j.scs.2023.104547

Bagheri, H., Sadjadi, S. Y., Sadeghian, S., 2014. Exploring the role of genetic algorithms and artificial neural networks for interpolation of elevation in geoinformation models. In Innovations in 3D Geo-Information Sciences (pp. 107–121). Springer.

Bagheri, H., Schmitt, M., Zhu, X. X., 2017a. Fusion of TanDEM-X and Cartosat-1 DEMs using TV-norm regularization and ANN-predicted weights. *2017 IEEE International Geoscience and Remote Sensing Symposium (IGARSS)*, IEEE, 3369–3372.

Bagheri, H., Schmitt, M., Zhu, X. X., 2017b. Uncertainty assessment and weight map generation for efficient fusion of TanDEM-X and Cartosat-1 DEMS. *The International Archives of the Photogrammetry, Remote Sensing and Spatial Information Sciences*, 42, 433–439.

Besharat, F., Dehghan, A. A., Faghih Khorasani, A., 2013. Empirical models for estimating global solar radiation: A review and case study. *Renewable and Sustainable Energy Reviews*, *21*, 798-821. https://doi.org/10.1016/j.rser.2012.12.043

Cucchiella, F., D'Adamo, I., Koh, S. L., 2015. Environmental and economic analysis of building integrated photovoltaic systems in Italian regions. *Journal of Cleaner Production*, *98*, 241-252. https://doi.org/10.1016/j.jclepro.2013.10.043

Dubayah, R., Rich, P., 1995. Topographic Solar Radiation Models for GIS. *International Journal of Geographical Information Systems*, *9*, 405-419. https://doi.org/10.1080/02693799508902046

Enerdata, 2018. *Global Energy Statistical Yearbook 2018*. https://yearbook.enerdata.net/electricity/electricity-domestic-consumption-data.html

Fu, P., 2000. The Solar Analyst 1. 0 User Manual. *Helios Environmental Modeling Institute, LLC*, *53*.

Heo, J., Jung, J., Kim, B., Han, S., 2020. Digital elevation model-based convolutional neural network modeling for searching of high solar energy regions. *Applied Energy*, *262*, 114588. https://doi.org/10.1016/j.apenergy.2020.114588

Hetrick, W., Rich, P., Barnes, F., Weiss, S., 1993. GIS-based solar radiation flux models. *American Society for Photogrammetry and Remote Sensing Technical Papers*, *3 GIS. Photogrammetry, and Modeling*, 132-143.

Hosseini, M., Bagheri, H., 2025. Improving the resolution of solar energy potential maps derived from global DSMs for rooftop solar panel placement using deep learning. *Heliyon*, *11*(1). https://doi.org/10.1016/j.heliyon.2024.e41193

Huang, H., Lin, L., Tong, R., Hu, H., Qiaowei, Z., Iwamoto, Y., Han, X.-H., Chen, Y.-W., Wu, J., 2020. *UNet 3+: A Full-Scale Connected UNet for Medical Image Segmentation*. https://doi.org/10.1109/ICASSP40776.2020.9053405

Huang, Y., Chen, Z., Wu, B., Chen, L., Mao, W., Zhao, F., Wu, J., Wu, J., Yu, B., 2015. Estimating roof solar energy potential in the downtown area using a GPU-accelerated solar radiation model and airborne LiDAR data. *Remote Sensing*, *7*(12), 17212-17233. https://doi.org/10.3390/rs71215877

Jung, J., Han, S., Kim, B., 2019. Digital numerical map-oriented estimation of solar energy potential for site selection of photovoltaic solar panels on national highway slopes. *Applied Energy*, *242*, 57-68. https://doi.org/10.1016/j.apenergy.2019.03.101

Kaba, K., Sarıgül, M., Avcı, M., Kandırmaz, H. M., 2018. Estimation of daily global solar radiation using deep learning model. *Energy*, *162*, 126-135. https://doi.org/10.1016/j.energy.2018.07.202

Kausika, B. B., Van Sark, W. G., 2021. Calibration and validation of ArcGIS solar radiation tool for photovoltaic potential determination in the Netherlands. *Energies*, *14*(7), 1865. https://doi.org/10.3390/en14071865

Kumari, P., Toshniwal, D., 2021. Deep learning models for solar irradiance forecasting: A comprehensive review. *Journal of Cleaner Production*, *318*, 128566. https://doi.org/10.1016/j.jclepro.2021.128566

Lee, M., Hong, T., Jeong, K., Kim, J., 2018. A bottom-up approach for estimating the economic potential of the rooftop solar photovoltaic system considering the spatial and temporal diversity. *Applied Energy*, *232*, 640-656. https://doi.org/10.1016/j.apenergy.2018.09.176

Li, Q., Krapf, S., Mou, L., Shi, Y., Zhu, X. X., 2024. Deep learning-based framework for city-scale rooftop solar potential estimation by considering roof superstructures. *Applied Energy*, *374*, 123839. https://doi.org/10.1016/j.apenergy.2024.123839

Miklánek, P., 1993. The estimation of energy income in grid points over the basin using simple digital elevation model. Annales Geophysicae,

Nelson, J. R., Grubesic, T. H., 2020. The use of LiDAR versus unmanned aerial systems (UAS) to assess rooftop solar energy potential. *Sustainable Cities and Society*, *61*, 102353. https://doi.org/10.1016/j.scs.2020.102353

Okolie, C., Adeleke, A., Mills, J., Smit, J., Maduako, I., Bagheri, H., Komar, T., Wang, S., 2024. Assessment of explainable tree-based ensemble algorithms for the enhancement of Copernicus digital elevation model in agricultural lands. *International Journal of Image and Data Fusion*, *15*(4), 430-460. https://doi.org/10.1080/19479832.2024.2329563

PDOK, 2024. *Dataset:CurrentHeightFileNetherlands(AHN)*. Retrieved 05.2024 from https://www.pdok.nl

Polo, J., García, R. J., 2023. Solar Potential Uncertainty in Building Rooftops as a Function of Digital Surface Model Accuracy. *Remote Sensing*, *15*(3), 567. https://www.mdpi.com/2072-4292/15/3/567

Prodanovic, D., 2002. Terrain Analysis – Principles and Applications, John P. Wilson, John C. Gallant (Eds.), Wiley, New York, 2000, 479 pp (index included), hbk, ISBN 0-471-32188-5. *Urban Water*, *4*. https://doi.org/10.1016/S1462-0758(01)00068-1

Ren, H., Xu, C., Ma, Z., Sun, Y., 2022. A novel 3D-geographic information system and deep learning integrated approach for high-accuracy building rooftop solar energy potential characterization of high-density cities. *Applied Energy*, *306*, 117985. https://doi.org/10.1016/j.apenergy.2021.117985

Ronneberger, O., Fischer, P., Brox, T., 2015. *U-Net: Convolutional Networks for Biomedical Image Segmentation* (Vol. 9351). https://doi.org/10.1007/978-3-319-24574-4_28

Shen, T., Zhou, T., Long, G., Jiang, J., Pan, S., Zhang, C., 2018. Disan: Directional self-attention network for rnn/cnn-free language understanding. Proceedings of the AAAI Conference on Artificial Intelligence.

Srećković, N., Lukač, N., Žalik, B., Štumberger, G., 2016. Determining roof surfaces suitable for the installation of PV (photovoltaic) systems, based on LiDAR (Light Detection And Ranging) data, pyranometer measurements, and distribution network configuration. *Energy*, *96*, 404-414. https://doi.org/10.1016/j.energy.2015.12.078

Šúri, M., Hofierka, J., 2004. A new GIS-based solar radiation model and its application to photovoltaic assessments. *Transactions in GIS*, *8*(2), 175-190. https://doi.org/10.1111/j.1467-9671.2004.00174.x

Wang, L., Wang, K., 2015. Impacts of DEM uncertainty on estimated surface solar radiation and extracted river network. *Bulletin of the American Meteorological Society*, *96*(2), 297-304. https://doi.org/10.1175/BAMS-D-13-00285.1

Zhong, Q., & Tong, D., 2020. Spatial layout optimization for solar photovoltaic (PV) panel installation. *Renewable energy*, *150*, 1-11. https://doi.org/10.1016/j.renene.2019.12.099

Zhong, T., Zhang, Z., Chen, M., Zhang, K., Zhou, Z., Zhu, R., Wang, Y., Lü, G., Yan, J., 2021. A city-scale estimation of rooftop solar photovoltaic potential based on deep learning. *Applied Energy*, *298*, 117132. https://doi.org/10.1016/j.apenergy.2021.117132